Conference Proceedings

Solar World Congress 2015
Daegu, Korea, 08 – 12 November 2015

Performance Analysis of Solar Tower Power Plants Driven Supercritical Carbon Dioxide Recompression Cycles for Six Different Locations in Saudi Arabia

Fahad A. Al-Sulaiman [1], Maimoon Atif[2] and Hafiz Abd-ur-rahman[2]

[1] Center of Research Excellence in Renewable Energy, Research Institute, King Fahd University of Petroleum & Minerals, Dhahran, 31261, (Saudi Arabia)

[2] Mechanical Engineering Department, King Fahd University of Petroleum & Minerals, Dhahran, 31261, (Saudi Arabia)

Abstract

In this study, thermodynamic analysis of supercritical carbon dioxide (sCO_2) recompression Brayton cycles integrated with solar thermal tower systems was carried out. First part of the model deals with generating a surround heliostat field layout. This heliostat field is then optimized for optical performance on annual basis using an evolutionary algorithm called the differential evolution. The other part of the model deals with modeling a recompression Brayton cycle, which uses the heat collected at the central receiver through the heliostat field. The developed mathematical model was implemented for six different locations (cities) in Saudi Arabia for comparative analysis. The selected cities were Tabouk (North), Madinah (West), Dhahran (East), Riyadh (Central), Bishah (South), and Najran (South). In addition, an auxiliary heat exchanger was also added before the expansion turbine to keep the turbine inlet temperature constant and, thus, to keep the net power output uniform. The target net power output was set to be 40 MW. The findings reveal that the highest annual average heat collected was for Madinah, 938,400 kWh/day, and the second highest was for Tabouk, 933,100 kWh/day. Consequently, the least amount of annual average fuel hybridization required was 5.82% for Madinah and 6.34% for Tabouk during daytime hours.

Keywords: *Solar tower power plant, supercritical CO_2, recompression Brayton cycle, hybrid solar power plant, heliostat optimization, Saudi Arabia*

1. Introduction

Solar tower or central receiver system comprises of a field of mirrors on the ground, which directs the solar radiation to a receiver mounted at the top of on a central tower. The receiver converts the solar radiation into heat and drives a thermodynamic cycle, which is usually a Brayton or a Rankine cycle, to generate power. Each individual mirror in the field is called a heliostat and it is equipped with a two-axes tracking system. As compared to parabolic troughs, solar towers can achieve higher temperature as more sunlight can be concentrated on a single receiver and the loss of heat can be minimized. Moreover, solar towers provide an opportunity to increase the capacity factor by using a thermal storage system and to maximize the power generated by allowing flexible generation strategy along with higher efficiency levels. With these advantages, A solar tower can be a tough competitor to parabolic trough in the future market with gained operating experience and reduced cost (IRENA, 2012).

In a study conducted by (Noone et al., 2012), a biomimetic pattern was proposed for the heliostat field layout. The model was based on the discretization of the heliostat surface for the calculation of the optical performance parameters, specifically the shading and blocking factor and the intercept factor. In their approach, a heliostat surface was divided into cells, however, this approach can be time consuming. (Besarati and Yogi Goswami, 2014) performed an optimization of the same biomimetic heliostat field pattern. In their study, a method was proposed to identify the potential shadowing and blocking heliostats for the calculation of the shading and

doi:10.18086/swc.2015.04.16 Available at http://proceedings.ises.org

blocking factor. Using their approach, a case study was carried out for the design of 50 MWth solar tower plant for Dagget, California.

A code called HFLCAL (Schmitz et al., 2006) was developed by the German Aerospace Center to optimize a heliostat field on annual basis. The code calculates the intercept by describing an analytical function, which computes the reflected image of each heliostat as a circular normal distribution. Their analysis was carried out for two latitude locations, i.e. 20° N and 40° N.

In a different study conducted by (Pitz-Paal et al., 2011), annual optimization of a heliostat field for solar to chemical energy conversion efficiency was performed for solar fuels production. The optimization was carried out by coupling genetic algorithm and the Nelder-Mead algorithm. It was concluded that the chemical process selected has a high impact on the basic design parameters and the performance. Furthermore, their study was carried out for a latitude location of 36.12°.

(Collado and Guallar, 2012) developed a code named Campo which takes into account thousands of heliostat co-ordinates for the optimization process. The code was validated in a different study (Collado and Guallar, 2013) using the literature data collected from Gemasolar (a solar tower power plant). In their study, more than desired number of heliostats was generated. Then optimization of the generated heliostat field was carried out by applying radial increments in the heliostat rows manually. And finally, the heliostats which had lower annual optical performance were eliminated to acquire the desired number of heliostats. Their study was carried out for Seville, Spain (latitude 37.46° N)

The Chinese Academy of Science developed a code for the heliostat field layout optimization called HFLD (Wei et al., 2010a, 2010b). In their code, the optimization was based on the receiver geometrical aperture and an efficiency factor. However, the intercept factor was calculated using the Monte Carlo ray tracing method. As a result, the accuracy will depend upon the number of rays traced and, consequently, this will result in a high computation time. Using this code, a new layout was also proposed for the PS10 power plant. Furthermore, this study was conducted for a latitude location of 40.4° N.

In a study by (Yao et al., 2009), a power plant was modeled using TRNSYS and integrated with HFLD (Wei et al., 2010a, 2010b) developed by the Chinese Academy of Science for the demonstration of 1 MW central receiver plant in Dahan, China. The basic flow calculation in the solar central receiver system and their integration to a plant were described. On the other hand, (Le Moullec, 2013) performed a techno-economic study on a coal fired power plant with a supercritical CO_2 Brayton cycle and a post combustion CO_2 capture mechanism. It was observed that the reduction of cost avoided CO_2 was 45% and the reduction in the levelized cost of electricity (LCOE) was 15%, without storage and transport, when compared to a reference supercritical coal fired power plant equipped with a standard carbon capture process.

The effect of a transient solar heat input on a supercritical CO_2 split expansion Brayton cycle was studied by (Iverson et al., 2013). They studied the performance of the turbomachinery in response to a fluctuating solar heat source. It was observed that the thermal mass in the system effectively enables the Brayton cycle to continue to run for short periods until the thermal input can recover.

It can be observed from the literature review that no study has been conducted when integrating a sCO2 recompression Brayton cycle with a solar thermal tower system accounting for the actual optical losses of the heliostat field. Furthermore, no study considers DE optimization technique for the optimization of the heliostat field on annual basis. In this article, a heliostat field was first generated for six selected locations (cities) in Saudi Arabia; and then these generated heliostat fields were optimized on annual basis while calculating all the necessary optical performance parameters of all the heliostats at every step of the optimization. The selection of the locations takes into consideration different potential geographical locations of the proposed solar power system. The locations selected for the analysis were Tabouk (North), Madinah (West), Dhahran (East), Riyadh (Central), Bishah (South) and Najran (South). Then, after calculating the heat collected through the solar thermal system for the selected cities, comparative performance analysis was carried out for the aforementioned cities. The results of the current research will be a valuable reference for both researchers and engineers in the solar thermal power field.

2. Mathematical modeling

A mathematical model was developed to achieve the objectives of the present study. The first part of the mathematical model deals with generating a preliminary heliostat field in a radial staggered configuration. The generated heliostat field is then tested for its optical performance, and there are five parameters which constitute the optical performance of the heliostat field layout namely the shadowing and blocking factor, the intercept factor, the atmospheric attenuation factor, the cosine factor, and the actual mirror reflectivity. The generated heliostat field is then optimized on annual basis using an evolutionary algorithm called the differential evolution (HFLODE: Heliostat Field Layout Optimization using Differential Evolution). Finally, a recompression Brayton cycle using sCO_2 as a working fluid was integrated with the solar thermal tower system with a net power output of 40 MW. Comparative performance analysis was carried out for six different locations nin Saudi Arabia while taking into account the direct normal incident irradiation for all of these locations.

2.1 Generating a heliostat field

The characteristic diameter is the distance between the center of the adjacent heliostats and it is defined by

$$DM = DH + dsep + x_1 \quad \text{(eq. 1)}$$

where DM is the characteristic diameter, DH is the heliostat diagonal and $dsep$ is any additional security distance between the heliostats. Here, x_1 is one of the optimizing parameters. By varying the value of this paramter, we can control the azimuthal spacing between the adjacent heliostats.

The minimum radial distance between the heliostat rows is equal to the height of an equilateral triangle and it is defined as

$$\Delta R_i = x_{2,i} DM \cos 30° \quad \text{(eq. 2)}$$

where $x_{2,i}$ is the second optimizing parameter and i denotes the zone of the heliostats. Using the parameter $x_{2,i}$ the radial spacing between the rows of the heliostats can be controlled and in turn the optical performance of the heliostats.

2.2 Solar positioning model

In order to calculate the instantaneous optical efficiency of the heliostat field, it is necessary to include a solar positioning model which can be defined as (Duffie and Beckman, 2013)

$$\delta = \frac{23.45\pi}{180} \sin\left(2\pi \frac{284 + n_d}{365}\right) \quad \text{(eq. 3)}$$

$$\omega_{sunrise} = \cos^{-1}(\tan\phi \tan\delta) - \pi = -\omega_{sunset} \quad \text{(eq. 4)}$$

$$\alpha_s = \sin^{-1}(\cos\phi \cos\delta \cos\omega_s + \sin\phi \sin\delta) \quad \text{(eq. 5)}$$

$$\gamma_s = \text{sgn}(\omega_s) \left| \cos^{-1} \frac{\sin\alpha_s \sin\phi - \sin\delta}{\cos\alpha_s \cos\phi} \right| \quad \text{(eq. 6)}$$

where δ is the solar declination angle, ω_s is the hour angle, n_d is the day of the year, ϕ is the latitude angle, α_s is the solar altitude, and γ_s is solar azimuth angle. Note that all angles are in radians.

2.3 Optical efficiency of the heliostat field

The total optical efficiency as defined by (Collado and Guallar, 2012) is

$$\eta_{opt}(x,y,t) = \rho \cos\omega(x,y,t) f_{at}(x,y) f_{sb}(x,y,t) f_{itc}(x,y,t) \quad \text{(eq. 7)}$$

where ρ is the reflectance of the heliostats, $\cos\omega$ is the incidence cosine between the incident sun ray and the normal to the heliostat surface, f_{sb} is the shadowing and blocking factor, f_{itc} is the intercept factor accounting for the fraction of the reflected rays intercepted by the receiver, and f_{at} is the atmospheric attenuation efficiency. Furthermore, x, y, and t represent the co-ordinates and time, respectively. The detail modeling of these five parameters was demonstrated in our previous study (Atif and Al-Sulaiman, 2015).

Tab. 1: Basic design and operating parameters used for the heliostat field and the central receiver (Collado and Guallar, 2013; Collado, 2008; Ho and Iverson, 2014)

Tower optical height, *THT*	130 m
Heliostat height , *LH*	9.75m
Heliostat width, *LW*	12.3m
Extra security distance, *dsep*	3m
Receiver diameter (cylindrical), *DR*	9.44
Receiver size, *LR*	9.44
Fraction of mirror area of heliostat	0.9642
Total number of heliostats	2646
Mirror reflectance × cleanliness, ρ	0.88 × 0.95
Standard deviation of sunshape errors,	2.51 mrad
Standard deviation of tracking errors,	0.63 mrad
Standard deviation of beam quality errors	1.88 mrad
Emittance of the receiver surface, ε	0.85
Absorptance of the receiver surface, α_R	0.95

2.4 Optimization of the heliostat field

The differential evolution is a population based optimization technique, which is characterized by its simplicity, robustness, few control variables, and fast convergence (Abido and Al-Ali, 2009). Because the DE technique is an evolutionary algorithm, it is suited for non-linear and non-differentiable optimization problems as well.

The strategy applied in this technique is to use the difference between randomly selected vectors to generate a new solution. For each solution in the original population, a trial solution is generated by performing the process of mutation, recombination, and selection operations. The old and new solutions are compared and the best solutions emerge in the next generation.

Furthermore, the DE in most instances as compared to the annealed Nelder and Mead approach, adaptive simulating annealing and the breeder genetic algorithm outperformed all of the aforementioned optimization techniques in terms of the required number of function evaluations necessary to locate a global optimum of the test functions (Storn and Price, 1997). Therefore, the DE was selected in this study.

The following equation is used for calculating the monthly averaged annual optical efficiency of the heliostat field:

$$\eta_{maa} = \frac{\sum_{j=1}^{12} \int_{t=sunrise}^{t=sunset} \eta_{opt} dt}{\sum_{j=1}^{12} \int_{t=sunrise}^{t=sunset} dt} \qquad \text{(eq. 8)}$$

where η_{maa} is monthly averaged annual heliostat field efficiency, the subscript *maa* denotes monthly annual averaged, and *j* denotes the average day of each month from January to December for the whole year as given in (Duffie and Beckman, 2013; Klein, 1977). This equation was used as the objective function for optimization.

2.5 Central receiver

The radiation heat losses, the convection heat losses and the optical losses were considered for the modeling of the central receiver as discussed next. The modeling of the central receiver was performed in EES. The equation for the radiation heat losses was given by (Sheu and Mitsos, 2013) as

$$Q_{rad} = F_{view} A_R \varepsilon \sigma T_R^4 \qquad \text{(eq. 9)}$$

where F_{view} is the radiation shape factor, A_R is the radiative area of the central receiver, ε is emissivity of the receiver, σ is the Stefan Boltzmann constant, and T_R is the receiver temperature.

The equation for convective heat losses from the central receiver is given as

$$Q_{conv} = A_R h_{conv} (T_R - T_{amb}) \qquad \text{(eq. 10)}$$

where h_{conv} is calculated by Bejan correlation for vertical chamber with natural convection and is defined as (Segal and Epstein, 1999)

$$h_{conv} = 0.557 \times 10^{-6} \left(\frac{T_R - T_{amb}}{H_t}\right)^{0.25} [\text{kW/ m}^2 - \text{K}] \qquad \text{(eq. 11)}$$

where H_t is the total height of the solar tower and T_{amb} is the ambient temperature.

where

$$Q_u = Q_{net} = \alpha_R Q_{in} - (Q_{rad} + Q_{conv}) \qquad \text{(eq. 12)}$$

$$Q_{in} = \eta_{opt} Q_{solar} \qquad \text{(eq. 13)}$$

$$Q_{solar} = I A_h \qquad \text{(eq. 14)}$$

Here, α_R is the absorptance of the receiver, I is the direct normal incident radiation, A_h is the total area of the heliostats, Q_u (or Q_{net}) is the net useful energy gained at the receiver, Q_{solar} is the total incident energy on the heliostat field, and Q_{in} is the net energy gained at the receiver.

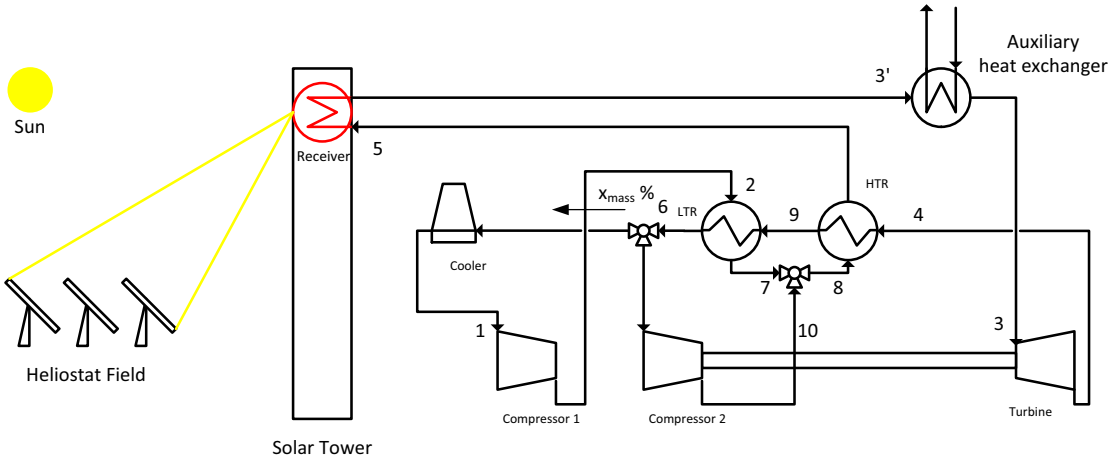

Fig. 1: Recompression closed loop supercritical carbon dioxide Brayton cycle with auxiliary heater

2.6 Closed loop sCO_2 recompression Brayton cycle

In a previous study by the authors (Al-Sulaiman and Atif, 2015), it was demonstrated that the recompression Brayton cycle demonstrated the highest thermal efficiency as compared to other Brayton cycles. Therefore, this cycle was selected for this study. In the recompression Brayton cycle (Figure 1), the flow is split into two streams after the low temperature regenerator and before passing through the cooler. These two streams are the one that flows to the main compressor through the cooler and the other one flows to the recompression compressor. Consequently, the system rejects less heat and the compressor work is reduced, which in turn causes the thermal efficiency to improve. The analysis of the Brayton cycle was also performed in EES and this code was integrated with the central receiver. The modeling of this cycle is presented as follows.

The power input of the first compressor is defined as

$$W_c = x_{mass}\dot{m}(h_2 - h_1) \qquad \text{(eq. 15)}$$

where x_{mass} is the fraction of the mass flow rate through the first compressor, $\dot{m}$ is the mass flow rate of sCO_2, and h is the specific enthalpy.

The power input of the second compressor is defined as

$$W_{c2} = (1 - x_{mass})\dot{m}(h_{10} - h_6) \qquad \text{(eq. 16)}$$

The useful energy gained at the receiver is defined as

$$Q_u = \dot{m}(h_3' - h_5) \qquad \text{(eq. 17)}$$

The heat added by the auxiliary heater is defined as

$$Q_{aux} = \dot{m}(h_3 - h_3') \qquad \text{(eq. 18)}$$

The turbine power can be defined as

$$W_T = \dot{m}(h_3 - h_4) \qquad \text{(eq. 19)}$$

Tab. 3: Basic design and operating parameters used for the sCO_2 recompression Brayton cycle

Temperature at the inlet of compressor (first compressor)	31.25° C
Turbine inlet temperature T_3 (*TIT*)	570° C
Pressure at the inlet of the compressor (first compressor)	7.4 MPa
Pressure ratio	2.7
Mass flow rate $\dot{m}$	469.2 kg/s
High temperature regenerator effectiveness (Chacartegui et al., 2011)	0.85
Low temperature regenerator effectiveness	0.7
Isentropic efficiencies of the compressors (Chacartegui et al., 2011)	0.8
Isentropic efficiency of the turbine (Chacartegui et al., 2011)	0.9
Thermal efficiency of the cycle η_{th}	0.4517
Net power output by the cycle	40079 kW ≈ 40 MW

Applying the energy balance on the high temperature regenerator to obtain

$$h_4 - h_9 = h_5 - h_8 \quad \text{(eq. 20)}$$

Applying the energy balance on the low temperature regenerator to obtain

$$x_{mass}(h_7 - h_2) = h_9 - h_6 \quad \text{(eq. 21)}$$

The energy rejected at the cooler is defined as

$$Q_{out} = x_{mass}\dot{m}(h_6 - h_1) \quad \text{(eq. 22)}$$

The net power output of the cycle is defined as

$$W_{net} = W_T - W_C - W_{C2} \quad \text{(eq. 23)}$$

The thermal efficiency of the cycle is given by

$$\eta_{th} = \frac{W_{net}}{Q_u + Q_{aux}} \quad \text{(eq. 24)}$$

The fraction of fuel hybridization required to keep a constant power output is given by

$$f_{hybrid} = \frac{Q_{aux}}{Q_{solar} + Q_{aux}} \quad \text{(eq. 25)}$$

The input solar share is defined as

$$X_{solar} = \frac{Q_{solar}}{Q_{solar} + Q_{aux}} \quad \text{(eq. 26)}$$

3, Results and discussion

In this study, a complete thermodynamic analysis of the solar thermal tower system integrated with a closed loop sCO_2 recompression Brayton cycle was performed. This analysis was carried out for six different locations in Saudi Arabia taking into account each of the locations' direct normal irradiation. The target net power output was 40 MW and the analysis was carried out in accordance with this net power output. This net power output was made uniform and for this purpose an auxiliary heat source was added. This plant would be operational with the input solar energy and auxiliary heat source for daylight hours; nonetheless, for nighttime operation the plant would operate on auxiliary heat source. Detailed analysis of the input solar share and the auxiliary heat provided has also been performed. Table 1 lists the design parameters of the heliostat and the central receiver which were used in this study whereas the operating conditions of the recompression sCO_2 Brayton cycle are listed in Table 2. Finally, in Table 3 the details of the cities including the latitude and longitude with the annual heat collected at the central receiver is provided.

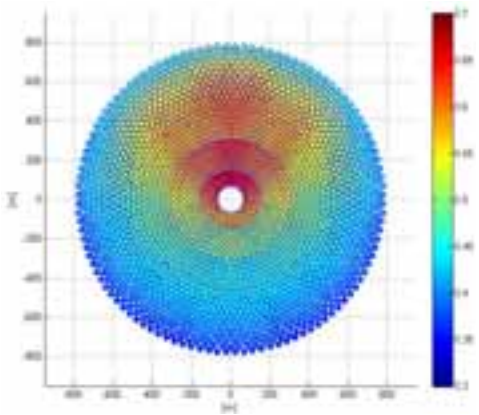

Fig. 2a Contours of the optical efficiency of the optimized heliostat field on annual basis for Tabouk, Saudi Arabia

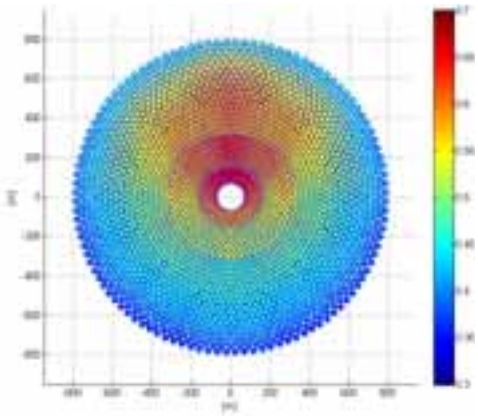

Fig. 2b: Contours of the optical efficiency of the optimized heliostat field on annual basis for Madinah, Saudi Arabia

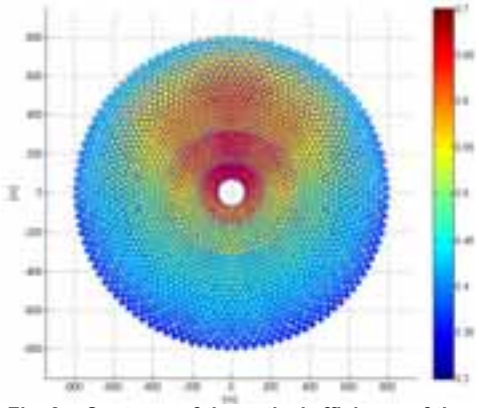

Fig. 2c: Contours of the optical efficiency of the optimized heliostat field on annual basis for Dhahran, Saudi Arabia

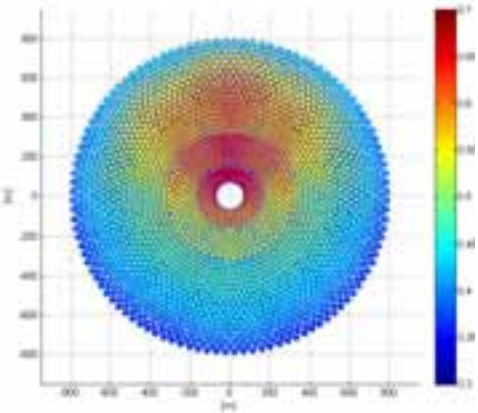

Fig. 2d: Contours of the optical efficiency of the optimized heliostat field on annual basis for Riyadh, Saudi Arabia

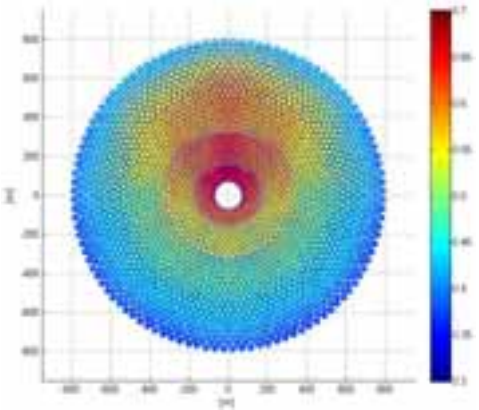

Fig. 2e: Contours of the optical efficiency of the optimized heliostat field on annual basis for Bishah, Saudi Arabia

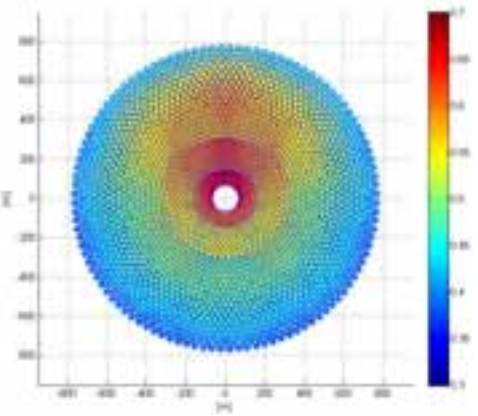

Fig. 2f: Contours of the optical efficiency of the optimized heliostat field on annual basis for Najran, Saudi Arabia

The solar resource data for each of the locations aforementioned was taken from a renewable energy resource website sponsored by NASA ("Surface meterology and Solar energy," n.d.). The data available on this website is averaged over a period of 22 years from 1983 until 2005. The averaged values over a month of direct normal irradiation are available there. A preliminary generated heliostat field was optimized on monthly averaged annual basis. Therefore, Equation 8 was used for the annual optimization for all the locations considered in this study. This code calculates all the necessary optical performance parameters of all the heliostats at every step of the optimization until the best layout of the generated heliostat field is found. The optimized heliostat fields for all of selected locations have been depicted in Figures 2a-2f.

As the data available on the aforementioned website was available on monthly basis, the average efficiencies of each month for all the locations were calculated after the heliostat fields were annually optimized. These efficiencies were used as an input to the EES code for the analysis of the receiver and recompression Brayton cycle. In this study; optical, convection heat, and radiation heat losses were taken into account, whereas the conduction heat losses were neglected from the receiver.

Figures 3a – 3f depicts bar graphs for the average heat collected for each month, for Tabouk, Madinah, Dhahran, Riyadh, Bishah, and Najran, respectively. Moreover, it can be observed that Madinah has the highest annual average heat collected in kWh/day (Table 3), whereas Tabouk has the second highest and Dhahran has the lowest. For Tabouk, Madinah, Dhahran, and Riyadh; the highest heat collected is in the month of June, whereas for Bishah and Najran it is not the case. Furthermore, it will be more preferable to install a plant where there are fewer fluctuations in the solar irradiation, such as Madinah (Figure 3b) and Bishah (Figure 3e). Such operating conditions will results in more stable operations. Therefore, the lifetime of the plant increases and its cost decreases.

A closed loop sCO_2 recompression Brayton cycle was integrated with the central receiver where the net heat collected was used as an input to the Brayton cycle. The modeling of the Brayton cycle was performed in such a way that heat gained at the receiver was used as an input value to the cycle rather than the turbine inlet temperature. Consequently, the temperature T_3' will not remain constant and will depend upon the irradiation of a particular location. Thus, the power output will not be uniform. To address this, an auxiliary heat exchanger was added before the turbine so that if the net heat gained at the receiver is low, extra heat will be added to keep the turbine inlet temperature constant and hence to keep the power output uniform. For this study, the turbine inlet temperature was fixed at 570° C and the net power output was fixed at 40MW. Figure 4 illustrate the percent hybridization required for all the cities during daylight hours. In other words, these bar graphs also show indirectly the amount of auxiliary heat required to keep a uniform power output in the daytime. From the figure, it can be observed that Madinah requires least amount of external fuel hybridization, i.e. only 5.82%, whereas Tabouk requires second least 6.34% and Najran requires third least i.e. 7.62%. During nighttime, the auxiliary boiler is working.

Tab. 3: Performance comparison of different locations of Saudi Arabia

City	Longitude	Latitude	Average annual heat collected at the central receiver (kWh/day)
Tabouk	36.5° E	28.5° N	933103
Madinah	39.5° E	24.5° N	938388
Dhahran	50.5° E	26.5° N	827420
Riyadh	46.5° E	24.5° N	855262
Bishah	42.5° E	20.5° N	882216
Najran	44.5° E	17.5° N	893359

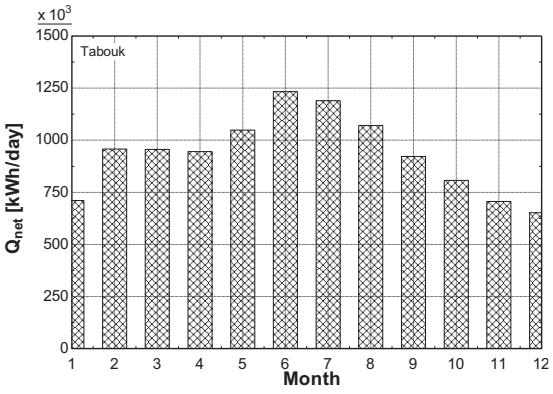

Fig. 3a: Average heat collected at the central receiver for Tabouk, Saudi Arabia

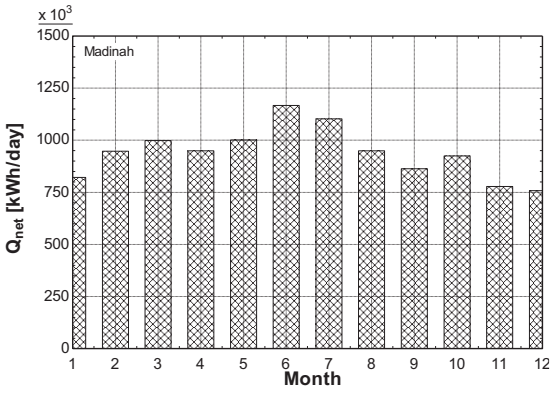

Fig. 3b: Average heat collected at the central receiver for Madinah, Saudi Arabia

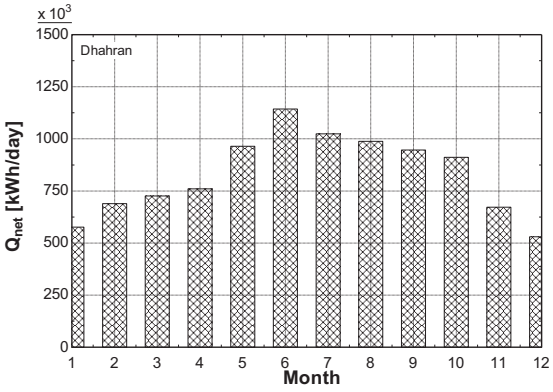

Fig. 3c: Average heat collected at the central receiver for Dhahran, Saudi Arabia.

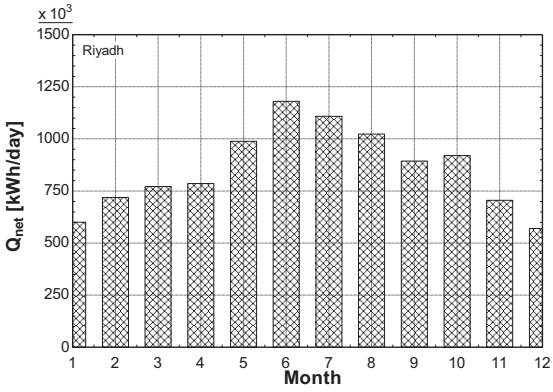

Fig. 3d: Average heat collected at the central receiver for Riyadh, Saudi Arabia.

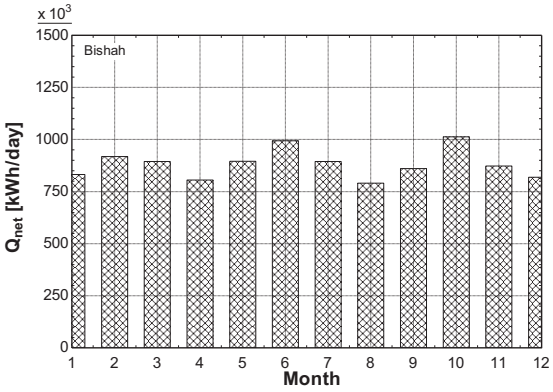

Fig. 3e: Average heat collected at the central receiver for Bishah, Saudi Arabia.

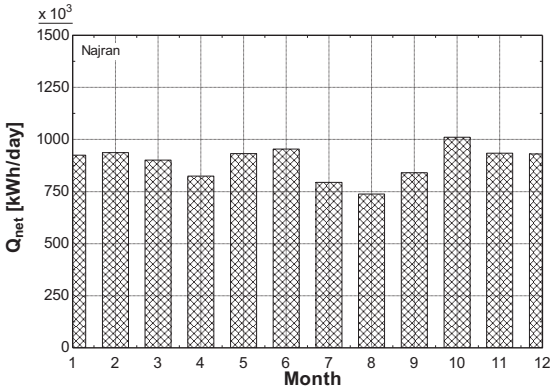

Fig. 3f: Average heat collected at the central receiver for Najran, Saudi Arabia.

4. Conclusions

A complete thermodynamic analysis of a solar thermal tower system when integrated with a sCO_2 recompression Brayton cycle was performed for six different locations in Saudi Arabia considering the local solar irradiation intensity for each location. The selected locations for the analysis were Tabouk (North), Madinah (West), Dhahran (East), Riyadh (Central), Bishah (South), and Najran (South). Heliostat fields were first generated and tested for their optical performance for these locations. The optical efficiencies of the generated heliostat fields were then optimized on annual basis considering all the optical performance parameters at every step of the optimization. A closed loop sCO_2 recompression Brayton cycle was then integrated with the central receiver where the heat is captured, which is reflected from the heliostat field. Furthermore, to keep the net power output uniform, an auxiliary heat exchanger was added before the expansion turbine. The findings indicated that the highest annual average heat collected was for Madinah (938,400 kWh/day) and the second highest was for Tabouk, (933,100 kWh/day). Similarly, the least amount of annual average fuel hybridization required was 5.82% for Madinah, and 6.34% for Tabouk during daytime.

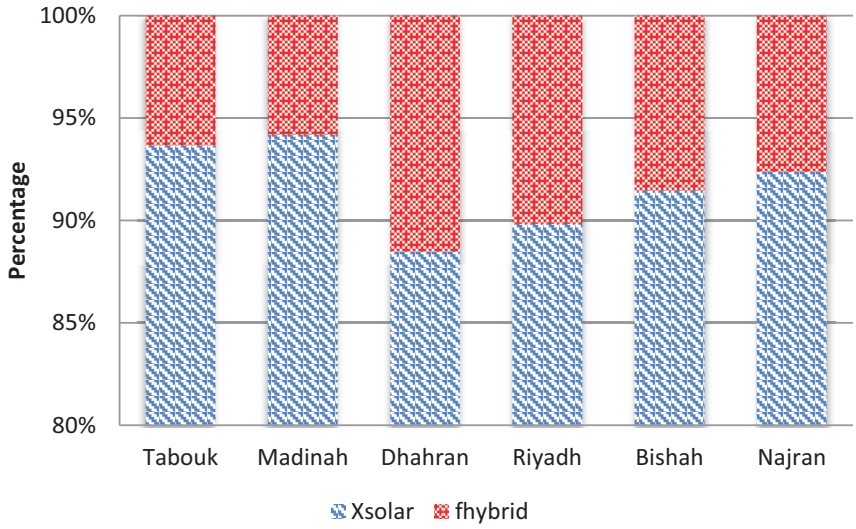

Fig. 4: Percentage of annual hybridization required for all of the locations considered.

Acknowledgement

The authors acknowledge the support of King Fahd University of Petroleum & Minerals (KFUPM), Dhahran, Saudi Arabia, for this work through project # SB121010.

References

Abido, M.A., Al-Ali, N.A., 2009. Multi-objective differential evolution for optimal power flow, in: 2009 International Conference on Power Engineering, Energy and Electrical Drives. IEEE, pp. 101–106. doi:10.1109/POWERENG.2009.4915212

Al-Sulaiman, F.A., Atif, M., 2015. Performance comparison of different supercritical carbon dioxide Brayton cycles integrated with a solar power tower. Energy 82, 61–71. doi:10.1016/j.energy.2014.12.070

Atif, M., Al-Sulaiman, F.A., 2015. Development of a mathematical model for optimizing a heliostat field layout using differential evolution method. Int. J. Energy Res. 39, 1241–1255. doi:10.1002/er.3325

Besarati, S.M., Yogi Goswami, D., 2014. A computationally efficient method for the design of the heliostat field for solar power tower plant. Renew. Energy 69, 226–232. doi:10.1016/j.renene.2014.03.043

Chacartegui, R., Muñoz de Escalona, J.M., Sánchez, D., Monje, B., Sánchez, T., 2011. Alternative cycles based on carbon dioxide for central receiver solar power plants. Appl. Therm. Eng. 31, 872–879. doi:10.1016/j.applthermaleng.2010.11.008

Collado, F.J., 2008. Quick evaluation of the annual heliostat field efficiency. Sol. Energy 82, 379–384. doi:10.1016/j.solener.2007.10.007

Collado, F.J., Guallar, J., 2013. A review of optimized design layouts for solar power tower plants with campo code. Renew. Sustain. Energy Rev. 20, 142–154. doi:10.1016/j.rser.2012.11.076

Collado, F.J., Guallar, J., 2012. Campo: Generation of regular heliostat fields. Renew. Energy 46, 49–59. doi:10.1016/j.renene.2012.03.011

Duffie, J.A., Beckman, W.A., 2013. Solar Engineering of Thermal Processes, Fourth Edi. ed. John Wiley & Sons, Inc., Hoboken, NJ, USA. doi:10.1002/9781118671603

Ho, C.K., Iverson, B.D., 2014. Review of high-temperature central receiver designs for concentrating solar power. Renew. Sustain. Energy Rev. 29, 835–846. doi:10.1016/j.rser.2013.08.099

IRENA, 2012. Renewable Power Generation Costs in 2012 : An Overview. Abu Dhabi, United Arab Emirates.

Iverson, B.D., Conboy, T.M., Pasch, J.J., Kruizenga, A.M., 2013. Supercritical CO2 Brayton cycles for solar-thermal energy. Appl. Energy 111, 957–970. doi:10.1016/j.apenergy.2013.06.020

Klein, S.A., 1977. Calculation of monthly average insolation on tilted surfaces. Sol. Energy 19, 325–329. doi:10.1016/0038-092X(77)90001-9

Le Moullec, Y., 2013. Conceptual study of a high efficiency coal-fired power plant with CO2 capture using a supercritical CO2 Brayton cycle. Energy 49, 32–46. doi:10.1016/j.energy.2012.10.022

Noone, C.J., Torrilhon, M., Mitsos, A., 2012. Heliostat field optimization: A new computationally efficient model and biomimetic layout. Sol. Energy 86, 792–803. doi:10.1016/j.solener.2011.12.007

Pitz-Paal, R., Botero, N.B., Steinfeld, A., 2011. Heliostat field layout optimization for high-temperature solar thermochemical processing. Sol. Energy 85, 334–343. doi:10.1016/j.solener.2010.11.018

Schmitz, M., Schwarzbözl, P., Buck, R., Pitz-Paal, R., 2006. Assessment of the potential improvement due to multiple apertures in central receiver systems with secondary concentrators. Sol. Energy 80, 111–120. doi:10.1016/j.solener.2005.02.012

Segal, A., Epstein, M., 1999. Comparative performances of `tower-top' and `tower-reflector' central solar receviers. Sol. Energy 65, 207–226. doi:10.1016/S0038-092X(98)00138-8

Sheu, E.J., Mitsos, A., 2013. Optimization of a hybrid solar-fossil fuel plant: Solar steam reforming of methane in a combined cycle. Energy 51, 193–202. doi:10.1016/j.energy.2013.01.027

Storn, R., Price, K., 1997. Differential Evolution – A Simple and Efficient Heuristic for global Optimization over Continuous Spaces. J. Glob. Optim. 11, 341–359. doi:10.1023/A:1008202821328

Surface meterology and Solar energy [WWW Document], n.d. URL https://eosweb.larc.nasa.gov/cgi-bin/sse/sse.cgi?skip@larc.nasa.gov

Wei, X., Lu, Z., Wang, Z., Yu, W., Zhang, H., Yao, Z., 2010a. A new method for the design of the heliostat field layout for solar tower power plant. Renew. Energy 35, 1970–1975. doi:10.1016/j.renene.2010.01.026

Wei, X., Lu, Z., Yu, W., Wang, Z., 2010b. A new code for the design and analysis of the heliostat field layout for power tower system. Sol. Energy 84, 685–690. doi:10.1016/j.solener.2010.01.020

Yao, Z., Wang, Z., Lu, Z., Wei, X., 2009. Modeling and simulation of the pioneer 1MW solar thermal central receiver system in China. Renew. Energy 34, 2437–2446. doi:10.1016/j.renene.2009.02.022